AD-A169 905 COLLECTION OF IONS IN THE STRATOSPHERE(U) AIR FORCE GEOPHYSICS LAB HANSCOM AFB MA C SHERMAN 09 DEC 85 AFGL-TR-85-0317 1/1

UNCLASSIFIED F/G 4/1 NL

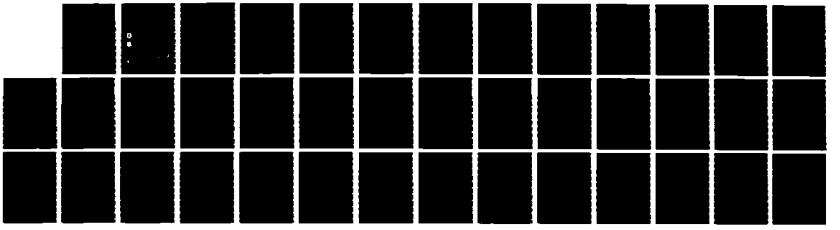

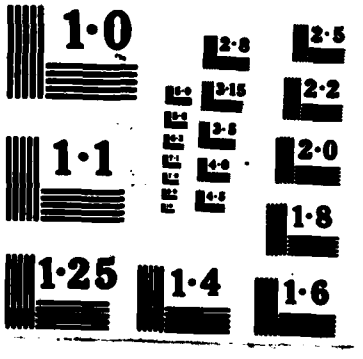
1·0
1·1
1·25
1·4
2·8
3·15
2·5
2·2
2·0
1·8
1·6

Collection of Ions in the Stratosphere

CHRISTOPHER SHERMAN

9 December 1985

IONOSPHERIC PHYSICS DIVISION PROJECT 2310
AIR FORCE GEOPHYSICS LABORATORY
HANSCOM AFB, MA 01731

This technical report has been reviewed and is approved for publication.

FOR THE COMMANDER

John E. Rasmussen

JOHN E. RASMUSSEN, Chief
Ionospheric Interactions Branch

Robert A. Skrivanek

ROBERT A. SKRIVANEK, Director
Ionospheric Physics Division

This document has been reviewed by the ESD Public Affairs Office (PA) and is releasable to the National Technical Information Service (NTIS).

Qualified requestors may obtain additional copies from the Defense Technical Information Center. All others should aply to the National Technical Information Service.

If your address has changed, or if you wish to be removed from the mailing list, or if the addressee is no longer employed by your organization, please notify AFGL/DAA, Hanscom AFB, MA 01731. This will assist us in maintaining a current mailing list.

Unclassified

SECURITY CLASSIFICATION OF THIS PAGE

AD-A169905

REPORT DOCUMENTATION PAGE

1a. REPORT SECURITY CLASSIFICATION: Unclassified	1b. RESTRICTIVE MARKINGS: None
2a. SECURITY CLASSIFICATION AUTHORITY	3. DISTRIBUTION/AVAILABILITY OF REPORT: Approved for public release; distribution unlimited
2b. DECLASSIFICATION/DOWNGRADING SCHEDULE	
4. PERFORMING ORGANIZATION REPORT NUMBER(S): AFGL-TR-85-0317 ERP, No. 944	5. MONITORING ORGANIZATION REPORT NUMBER(S)
6a. NAME OF PERFORMING ORGANIZATION: Air Force Geophysics Laboratory; 6b. OFFICE SYMBOL (If applicable): LIS	7a. NAME OF MONITORING ORGANIZATION
6c. ADDRESS (City, State and ZIP Code): Hanscom AFB Massachusetts 01731	7b. ADDRESS (City, State and ZIP Code)
8a. NAME OF FUNDING/SPONSORING ORGANIZATION; 8b. OFFICE SYMBOL (If applicable)	9. PROCUREMENT INSTRUMENT IDENTIFICATION NUMBER
8c. ADDRESS (City, State and ZIP Code)	10. SOURCE OF FUNDING NOS

PROGRAM ELEMENT NO.	PROJECT NO.	TASK NO.	WORK UNIT NO.
61102F	2310	G3	16

11. TITLE (Include Security Classification): Collection of Ions in the Stratosphere

12. PERSONAL AUTHOR(S): Christopher Sherman

13a. TYPE OF REPORT	13b. TIME COVERED	14. DATE OF REPORT (Yr., Mo., Day)	15. PAGE COUNT
Scientific Interim	FROM 9/84 TO 9/85	1985 December 9	42

16. SUPPLEMENTARY NOTATION

17. COSATI CODES			18. SUBJECT TERMS (Continue on reverse if necessary and identify by block number)
FIELD	GROUP	SUB GR	Stratospheric sampling
04	01		

19. ABSTRACT (Continue on reverse if necessary and identify by block number)

The processes involved in sampling of ions in the stratosphere have been examined and ranked in order of importance. Several typical calculations related to collection of ions in the stratosphere have been made. In this procedure, difficulties that may arise in solving such problems have been pointed out. The overall program, if continued, would be strengthened by further theoretical support along the lines initiated here.

20. DISTRIBUTION AVAILABILITY OF ABSTRACT	21. ABSTRACT SECURITY CLASSIFICATION
UNCLASSIFIED UNLIMITED ☒ SAME AS RPT ☐ DTIC USERS ☐	Unclassified

22a. NAME OF RESPONSIBLE INDIVIDUAL	22b. TELEPHONE NUMBER (Include Area Code)	22c. OFFICE SYMBOL
Christopher Sherman	617-861-2525	LIS

DD FORM 1473, 83 APR EDITION OF 1 JAN 73 IS OBSOLETE

Unclassified

SECURITY CLASSIFICATION OF THIS PAGE

Preface

In the fall of 1979, a program of balloon-borne mass spectrometric measurements was commenced at this laboratory. This work has been continued up to the present time, but little support in the way of theory has been undertaken. The present work is addressed towards making a start in this direction; it deals with the problems encountered in relating measured quantities to number densities of stratospheric ionic and neutral species.

I thank Pat Bench for programming the numerical solutions and Tony Quesada for bringing several useful references to my attention.

Contents

Illustrations

Collection of Ions in the Stratosphere

1. INTRODUCTION

1.1 Hierarchy of Time Constants

The problem of sampling in the atmosphere is that of finding how the number densities and fluxes of species we collect relate to the undisturbed ambient quantities. The nature of the problem will vary widely depending on the altitude regime considered. Here we consider collection using a balloon to carry the experiment in the regime between 20 and 40 km, so that continuum conditions may be taken to prevail. We envision the sampling to occur through a small orifice but do not follow the flow through the orifice. Instead, we ask the question: In the absence of the orifice, what is the flux of charged particles, here predominantly positive and negative ions, to the collecting surface in terms of the ambient number densities?

What happens to particles on entry into the detecting orifice and further into a detecting instrument is a separate problem of interest in its own right.

In this report, we do not undertake detailed calculations of the complicated geometries actually utilized. Rather, we discuss the collection process in general terms to assess the relative importance of the various processes involved, and, with an eye to these processes, we solve some relevant prototypical problems for simple geometries.

(Received for publication 9 December 1985)

There are, to begin with, three transport processes involved in the collection of charged particles in the stratosphere: bulk fluid flow, diffusion, and, if electric fields are present, mobility effects. To estimate the relative importance of these effects as well as to compare them with other non-transport processes, we develop a hierarchy of time constants, τ_i. First, we deal with the time constant for bulk fluid flow. This is given by a characteristic length L, divided by a velocity u_o. Now, the balloon itself moves with the ambient wind and velocities relative to the sampling platform are generated either by horizontal gradients or by local fluctuations in wind speed. If we take $3 < L < 100$ cm and $10 < u_o < 100$ cm/sec, we have $0.03 < \tau_B < 10$ sec where the subscript B refers to bulk flow.

For diffusion, typical time constants are ordinarily taken to be

$$\tau_D = \frac{L^2}{4D} = \frac{3}{4}\frac{L^2}{\lambda \bar{v}}$$

where D = the diffusion coefficient, λ = the mean free path, and $\bar{v}$ = root mean square thermal velocity. In the present instance, however, this formula may not be valid. Bulk flow across a surface creates a boundary layer, and, in the absence of diffusion, the number densities at the free edge of the boundary are the undisturbed values. The characteristic dimension for diffusion for transport across this layer then becomes the boundary layer thickness $\delta = L/\sqrt{Re}$ where Re is the bulk flow Reynolds number. We have then,

$$\tau_D = \frac{3}{4}\frac{L^2}{\lambda \bar{v} Re} = \frac{3}{4}\frac{L^2 \mu}{\lambda \bar{v} u_o \rho L}$$

(μ is the coefficient of viscosity, ρ the density)

and putting $\mu = \frac{1}{3}\lambda \rho \bar{v}$,

$$\tau_D = \frac{1}{4}\frac{L}{u_o}$$

We thus see that the range of τ_D is of the same order as that of τ_B. This is an interesting result. It implies that, although isolated diffusive times may be long compared to isolated bulk flow times, once bulk flow occurs, it enhances diffusion speeds so that these latter "keep step" with flow, as far as order of magnitude of influence is concerned; and further, that this occurs independently of altitude. If this interpretation is correct, great caution must be used before neglecting diffusive effects as being "small" in the sampling process.

We next consider the time constants associated with mobility phenomena. The

ratio of mobility times to diffusion times is given by

$$\frac{\tau_M}{\tau_D} = \left(\frac{L}{kE}\right)\left(\frac{4D}{\delta^2}\right) \cong \left(\frac{L^2}{k\phi_o}\right)\left(\frac{\lambda\bar{v}}{\delta^2}\right)$$

$$\cong \frac{\lambda\bar{v}}{k\phi_o}\,Re \cong \frac{\lambda\bar{v}}{e\lambda\phi_o}\,m\bar{v}\,Re = \frac{m\bar{v}^2}{e\phi_o}\,Re$$

Here κ, E, ϕ_o, e, and m are the mobility coefficient, electric field, electric potential, electronic charge, and particle mass, respectively. We take ϕ_o to lie between 1 and 20 V (typical collecting voltages), and take L = 10 cm and v_o = 30 cm/sec. We have

$$Re = \frac{\rho v_o L}{\mu} = \frac{\rho}{\rho_o}\left(\frac{\rho_o v_o L}{\mu}\right) = \frac{\rho}{\rho_o}\,\frac{300}{0.15} = 2000\,\frac{\rho}{\rho_o}$$

where ρ_o is the density at sea level, and

Alt (km)	ρ/ρ_o	Re	$m\bar{v}^2/e$ (V)	ϕ (V)	τ_M/τ_D
20	1/20	100	1/25	1	4.0
40	1/400	5	1/25	20	0.01

Thus, the range of τ_M overlaps the range of τ_D. This completes the estimates of transport times.

Finally, we turn to the question of generation and recombination times. Since the charged particle number density n_o, the generation rate q, and the recombination rate α are connected by $n_o = \sqrt{q/\alpha}$, the generation and recombination times are identical and are given by $\tau_G = \tau_R = (\alpha q)^{-1/2}$. We then have the following:

Alt (km)	q (cm^{-3} sec^{-1})	α (cm^3 sec^{-1})	n_o (cm^{-3})	τ_G, τ_R
20	15	5×10^{-7}	~5500	360
40	0.75	5×10^{-8}	~4000	5200

Thus, $\tau_G, \tau_R >> \tau_B, \tau_D, \tau_M$

We are now in position to state that when we collect ions in the stratosphere, the effects of bulk flow, diffusion, and mobility tend to dominate those of generation and recombination. Although the latter two establish the equilibrium number densities, it will often be possible to fix n_o as a boundary condition in the collection process.

1.2 Space Charge

In considering the effects of space charge, it is expedient to think in terms other than those of time constants.

Any biased collecting system (probe) placed in a plasma generates space charge (that is, separation of charges). If, however, the distribution of charge is such that the changes induced in the primary field are small, the primary field may be used to obtain collected currents, a much simpler problem than the self-consistent solution for fields and fluxes. The criterion as to when such approximation is permissible is, in general, connected with the Debye length λ_D. If $\lambda_D < L$, then space charge effects tend to be either dominant or at least substantial; while if $\lambda_D >> L$, they are small or negligible. In the present instance, the Debye length for the stratosphere is of the order of 2 cm, while material dimensions, L, are such that $10 < L < 100$ cm. The indications are thus that space charge effects will be substantial.

It is known, however, that the ratio of Debye length to material dimension is not the only dimensionless parameter related to space charge effects. A second and independent characteristic length $\lambda_S = \phi_o \varepsilon_o / n_o L e$, where ε_o is the permittivity of free space, may also be formed. The independence of λ_S from λ_D is obvious; λ_D contains only parameters related to plasma properties, while both ϕ_o and L are boundary properties.

The ratio γ_S/L is the reciprocal of the ratio of secondary (that is, space charge generated) electric fields to primary electric field. Thus, for the secondary field, E_S, we have on dimensional grounds,

$$E_S = \frac{n_o e L}{\varepsilon_o} \quad \text{and}$$

$$\frac{E_S}{E_o} = \frac{n_o e L^2}{\varepsilon_o \phi_o} = \frac{L}{L_S}$$

This dimensionless ratio may be expressed in terms commonly appearing in probe theory

$$\frac{E_S}{E_o} = \frac{L^2}{\lambda_D^2} \left(\frac{e\phi_o}{kT} \right)^{-1}$$

where k is Boltzmann's constant, and T is the temperature.

For $n_o = 5 \times 10^9/m^3$,

$$\frac{E_S}{E_o} = \frac{80\,L^2}{\phi_o}$$

Taking $L = 1\,m$ and $\phi_o = 1\,V$,

$$\frac{E_S}{E_o}_{MAX} = 80$$

while for $L = 0.1\,m$ and $\phi_o = 20\,V$

$$\frac{E_S}{E_o}_{MIN} = 0.04$$

This seems to indicate that under some conditions space charge will not play an important role in collection. This conclusion is the opposite of that drawn on the basis of Debye length considerations.

Although resolution of the role of space charge is not a minor matter, including space charge would lead into the domain of continuum probe theory, an endeavor that cannot be pursued here. We confine our calculations to those that ignore space charge.

1.3 Geometry

The overall geometry of the balloon platform and of the environs of the mass spectrometer entrance aperture are so complex that a very detailed numerical calculation would be required to treat the full surface boundary properly. Here, we consider two highly simplified aspects of the collection problem. In Section 3, we consider a possible effect on collection of the presence of the whole platform taken to be a sphere, in the presence of diffusion, generation, and recombination of charged particles. In Section 2, we consider a two-dimensional rectangular geometry in the immediate vicinity of the instrument entrance aperture. There is a possible application for this model calculation. This is an attempt to gain control of the sampling by creating a bulk flow sufficient to dominate random fluctuations present in ambient winds (Figure 1-1). The idea is that, by controlling the location of the housing and the speed of the bulk flow induced by the fan as well as the electric field intensity, the collection rate may be made independent of the ambient winds. At the same time, again by proper control of entry conditions, it should be possible to avoid contamination arising in the control surface itself.

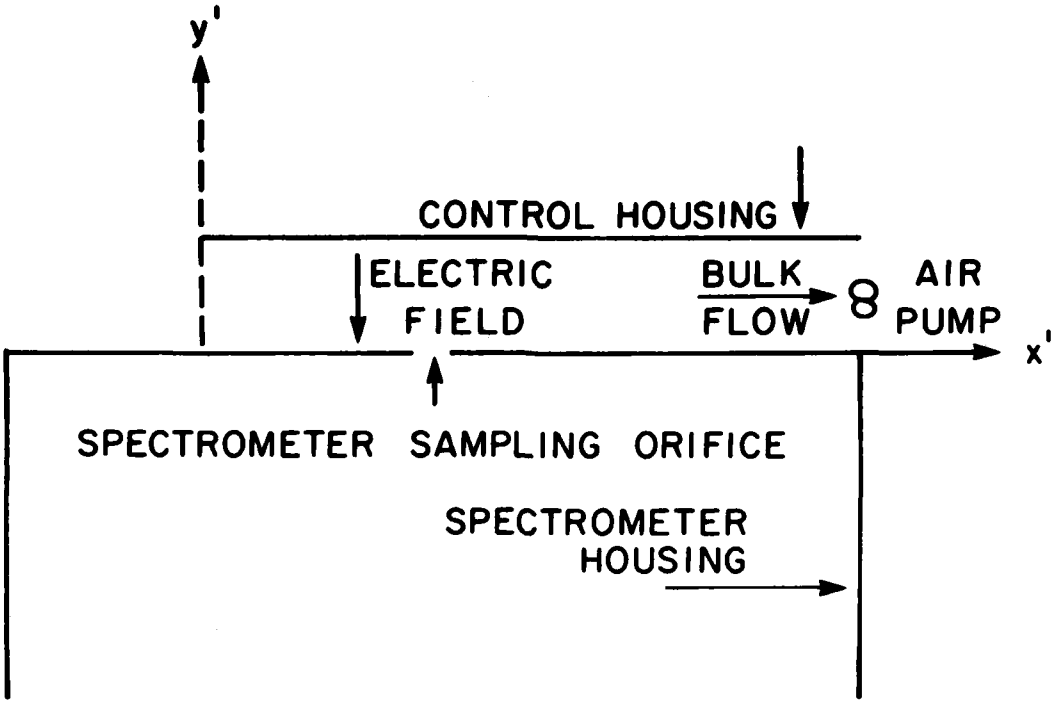

Figure 1-1. Schematic Representation of Simplified Collecting System

The calculations done in Section 2 are preliminary to a model for such a collection system.

2. DIFFUSION, MOBILITY, AND FLOW WITH RECTANGULAR GEOMETRY

2.1 Series Solution

In this section, we solve a simple boundary value problem involving diffusion, bulk flow, and mobility. Under conditions for which a definite known mobility law is valid and there is also no space charge, there is then no real distinction between bulk and mobility flows. The electric field is solved for as a separate problem, and the total flow field resulting from both electrical and mechanical forces is then a known function that is inserted into the continuity equation.

One of the purposes of this calculation is to illustrate the role that diffusion may play in modifying both density distributions and fluxes. It is often taken for granted that, in the presence of substantial flow fields, diffusion effects may be neglected. This is universally done, for example, in the discussion of Gerdien

condensers. In fact, diffusion may play a significant role in ion collection even when the pertinent dimensionless parameters indicate that flow dominates diffusion.

A further reason for including diffusion in sampling calculations is to obtain consistency in the application of boundary conditions to the relevant differential equations. Diffusion equations are of higher order than inviscid flow equations and thus permit the specification of ion number densities on both collecting and other surfaces (or at infinity). This cannot be done when diffusion is neglected.

The boundary value problem we investigate here will be solved in three ways: (1) by a series solution; (2) by a numerical machine solution; and (3) by a singular perturbation method. These three methods are complementary and contribute to the evaluation of validity of numerical solutions, a benefit in extending the solutions to situations that cannot be solved analytically.

The continuity equation for number density of ions, n', undergoing diffusion, bulk flow, and mobility effects is

$$\vec{\nabla} \cdot \left[n' \left(\vec{u} + \mu \vec{E} \right) - D \vec{\nabla} n' \right] = 0 \tag{2-1}$$

where $\vec{u}$ is the bulk flow velocity, and, in this section, μ is the mobility coefficient, $\vec{E}$ the electric field, and D the diffusion coefficient. If we assume that D is constant, we have

$$n' \vec{\nabla} \cdot \left(\vec{u} + \mu \vec{E} \right) + \left(\vec{u} + \mu \vec{E} \right) \cdot \vec{\nabla} n' - D \nabla^2 n' = 0 \tag{2-2}$$

For incompressible flow and no space charge, $\vec{\nabla} \cdot \vec{u} = \vec{\nabla} \cdot \vec{E} = 0$. Further, we let $\vec{u} = u_x (y)$ and $\mu \vec{E} = \vec{v} = v_y$ (see Figure 1-1) so that

$$D \nabla^2 n' - u \frac{\partial n'}{\partial x'} - v \frac{\partial n'}{\partial y'} = 0 \tag{2-3}$$

Now, letting the separation between the housing plates be L, and using rectangular coordinates, set

$$y = y'/L, \; x = x'/L, \; n = n'/n_o$$

Then

$$\frac{\partial^2 n}{\partial x^2} + \frac{\partial^2 n}{\partial y^2} - \sigma \frac{\partial n}{\partial x} - \rho \frac{\partial n}{\partial y} = 0 \tag{2-4}$$

where

$$\sigma = \frac{uL}{D}$$

and in this section, we use a different definition of ρ,

$$\rho = \frac{vL}{D}$$

and n_o is the ambient ion density. The boundary conditions for this problem are:

$$n(x, 0) = n(x, 1) = 0 \tag{2-5}$$

$$n(0, y) = 1 \tag{2-6}$$

$$n(\infty, y) = 0 \tag{2-7}$$

Now, let $u = u_x$ and $v = v_y$ be constants. Then the Eq. (2-4) is separable, and, for the given boundary conditions, the solution (details of which are omitted) is

$$n = 8\pi \exp\left(\frac{\sigma x + \rho y}{2}\right) \sum_{j=1}^{\infty} \exp\left[-(\sigma^2 + \rho^2 + 4\pi^2 j^2)^{1/2} \frac{x}{2}\right] \frac{j}{\rho^2 + 4\pi^2 j^2}$$

$$* \left[1 + (-1)^{j+1} e^{-\rho/2}\right] \sin \pi j y \tag{2-8}$$

To find the flux to the collecting surface $y = 0$, we reintroduce the primes which designate the original dimensional variables. We have

$$\text{Flux} = F' = -D\vec{\nabla}' n' \Big|_{y'=o} = -D \frac{\partial n'}{\partial y'} \Big|_{y'=o} = -\frac{D}{L} n_o \frac{\partial n}{\partial y} \Big|_{y=o} \tag{2-9}$$

Let $F = F'/n_o v$. Then

$$F = -\frac{D}{LV} \frac{\partial n}{\partial y} = -\frac{1}{\rho} \frac{\partial n}{\partial y} \tag{2-10}$$

F is the non-dimensional ratio of the observed flux to the diffusion-free flux. We have

$$-\rho F = 8\pi^2 \, e^{\sigma/2\, x} \sum_{j=1}^{\infty} \exp\left[-(\sigma^2 + \rho^2 + 4\pi^2 j^2)^{1/2} \frac{x}{2}\right] \frac{j^2}{\rho^2 + 4\pi^2 j^2}$$

$$* \left[1 + (-1)^{j+1} \, e^{-\rho/2}\right] \qquad (2\text{-}11)$$

We note that, with our choice of coordinate axes and flow directions, u and v are positive and negative respectively; hence, in Eqs. (2-8) and (2-11) (and in general herein), σ and ρ are also positive and negative respectively.

The utility of Eqs. (2-8) and (2-11) depends to a large extent on rates of convergence, and this latter clearly depends, in turn, on values of σ and ρ. If we assume that $O[\sigma] = O[-\rho]$, it is seen that both the summed exponential and $(\rho^2 + 4\pi^2 j^2)^{-1}$ terms start to decrease when $O[j] = \rho/2\pi$. Thus, to obtain convergence, we must have $O[jMAX] >> \rho/2\pi$, where jMAX is the terminal value of j in the sum.

This, however, is only a necessary, not a sufficient, condition for these equations to represent valid solutions; for we must guarantee not only that the series converges, but that, in a practical sense, it converges to correct values. If the series is summed by digital computer, we may expect approximately 12-place accuracy. When $O[\sigma] = O[-\rho] \cong 100$, initial terms in the series ($O[j] \cong 1$) are of order

$$\frac{8\pi}{\rho^2} \exp\left\{\frac{\sigma}{2}\left[1 + \frac{x}{2}(1 - \sqrt{2})\right]\right\}$$

which, depending on the value of x, may be as great as $\sim 10^{17}$. Since, for n, the correct converged values must be ≤ 1, it is clear that for such large values of σ and $-\rho$, the series sum will be meaningless, even though the series converges. Actual summing bears these ideas out. At $\sigma = -\rho = 80$, the results are without meaning; at $\sigma = -\rho = 60$, the results appear to be valid. Thus, a practical limit is set on the range of values of σ and $-\rho$ for which this series solution can be utilized.

Because of the limitations on use of the series solution, it is important to know what range of values of σ and ρ to expect in practice. For this purpose, we choose u, $-v \cong 10$ m/sec and L = 1 m as upper limits, and u, $-v \cong 1$ m/sec, L = 0.1 m as lower, we thus obtain (using values of λ from Appendix C)

	20 km	40 km
σ_{MAX}	5000	250
σ_{MIN}	50	2.5

The range of σ thus includes both values which can and cannot be summed in series form. This points up the need for alternative solutions.

We now present graphically some of the results obtained from Eqs. (2-8) and (2-11). Figure 2-1 shows fluxes, $-\rho F$, both with and without diffusion, as a function of x, with $\sigma = -\rho$ as a parameter. Even at $\sigma = 60$, there are still substantial

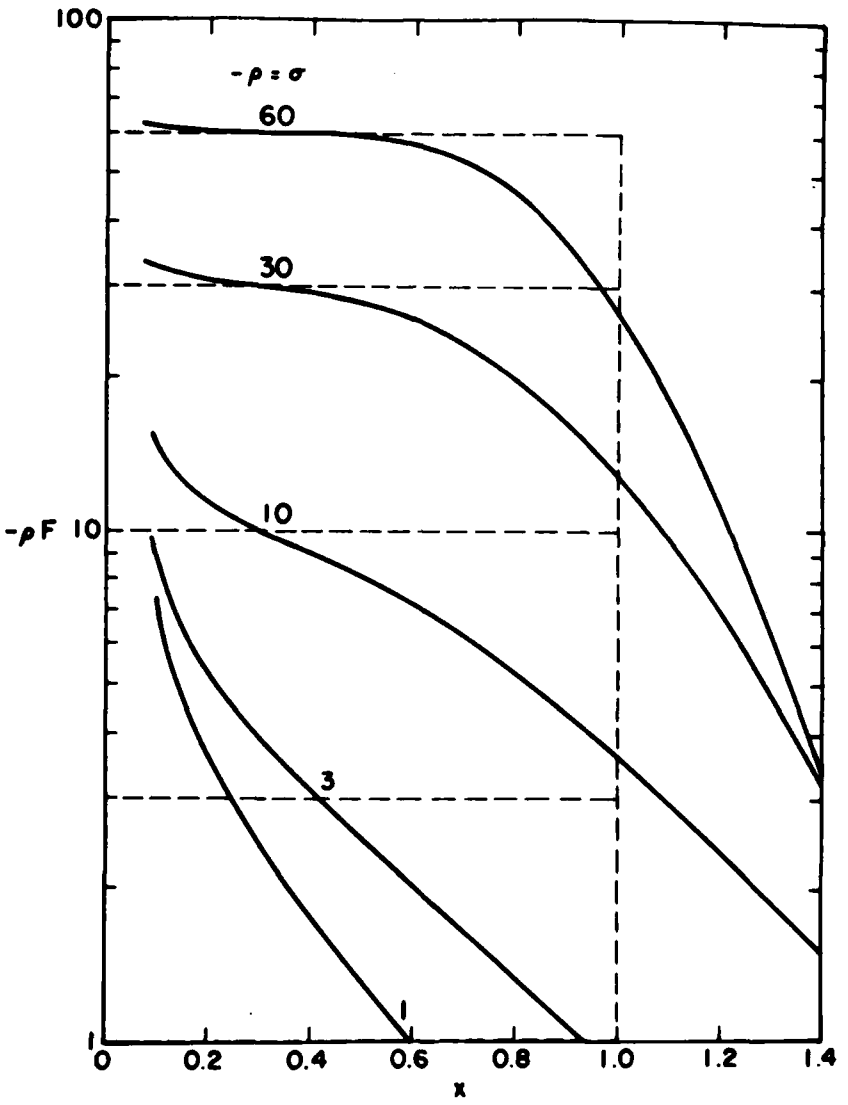

Figure 2-1. Normalized Flux $-\rho F$ vs x, With $-\rho = \sigma$ as a Parameter. Solid lines are obtained from series solution; dashed, solution without diffusion

influences due to the presence of diffusion. (In looking at these graphs, the values of flux near $x = 0$, showing an actual or incipient increase, need cause no concern. This increase is an artifact due to the singularity in boundary conditions at $x = y = 0$.) Figure 2-2 shows fluxes $-\rho F$ as a function of σ for $\rho = -30$ and three locations x again with the corresponding diffusionless cases, also shown in dashed lines. The approach to the diffusionless case ($-\rho F = 30$ for $x < -\sigma/\rho$; $-\rho F = 0$ for $x > -\sigma/\rho$) with increasing values of σ is seen.

Figures 2-3 and 2-4 show number densities as functions of x and y, respectively, for $\sigma = -\rho = 10.0$ obtained by summing Eq. (2-8). The corresponding diffusionless series have not been drawn in, but, as might be expected with $\sigma = -\rho = 10$, the solutions with diffusion differ very substantially from those without.

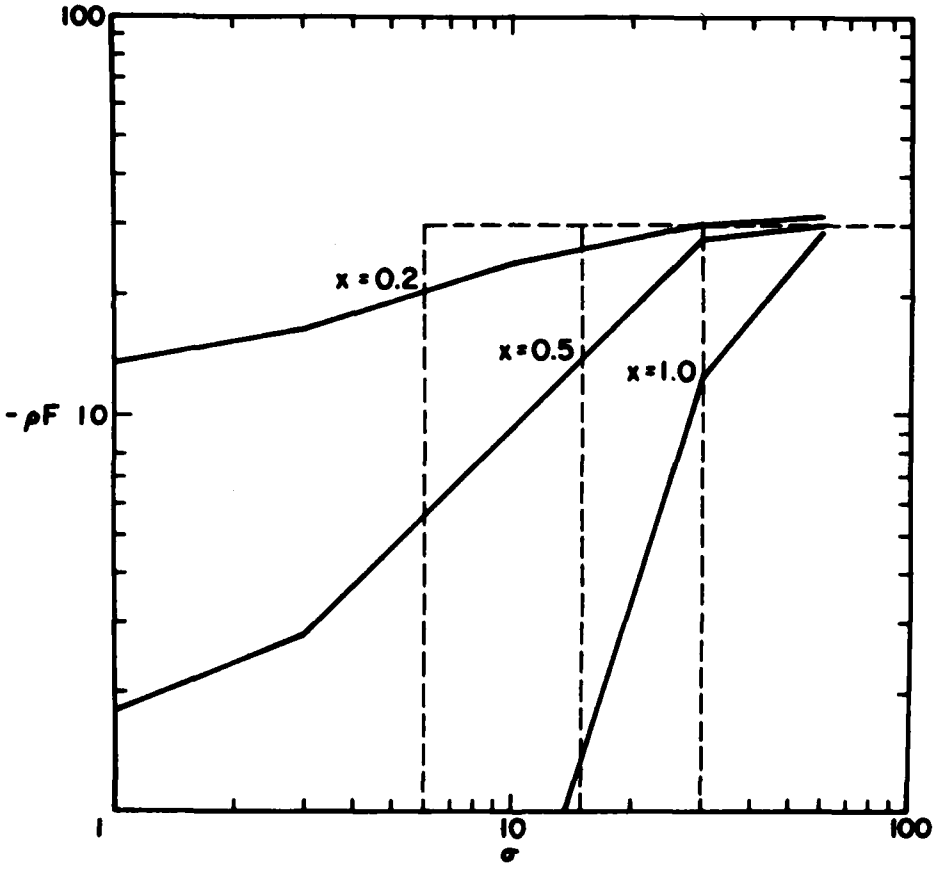

Figure 2-2. Normalized Flux $-\rho F$ vs σ, With x as a Parameter and $-\rho = 30$. Solid lines are obtained from series solution; dashes, without diffusion

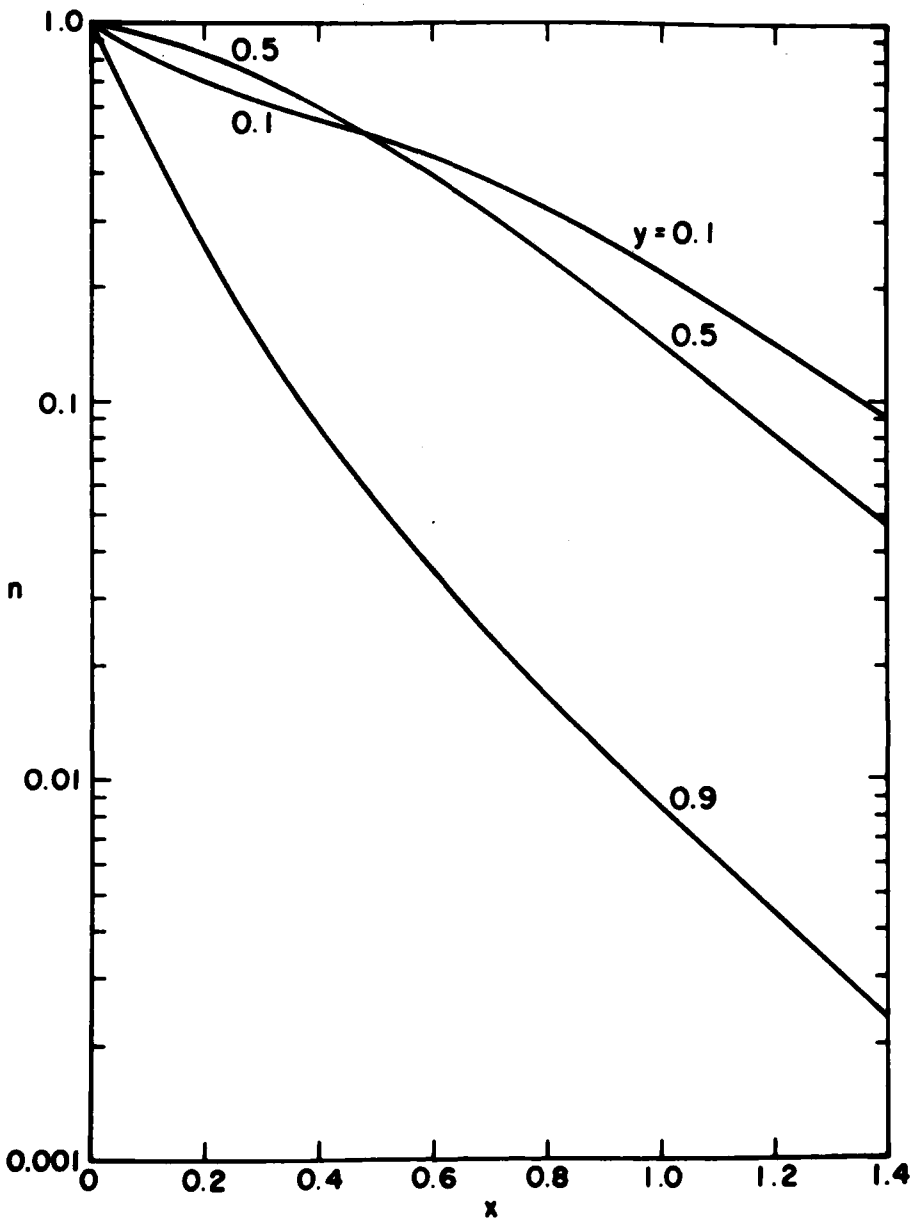

Figure 2-3. Number Density n, vs x With y as a Parameter and $-\rho = \sigma = 10.0$ as Obtained From Series Solution

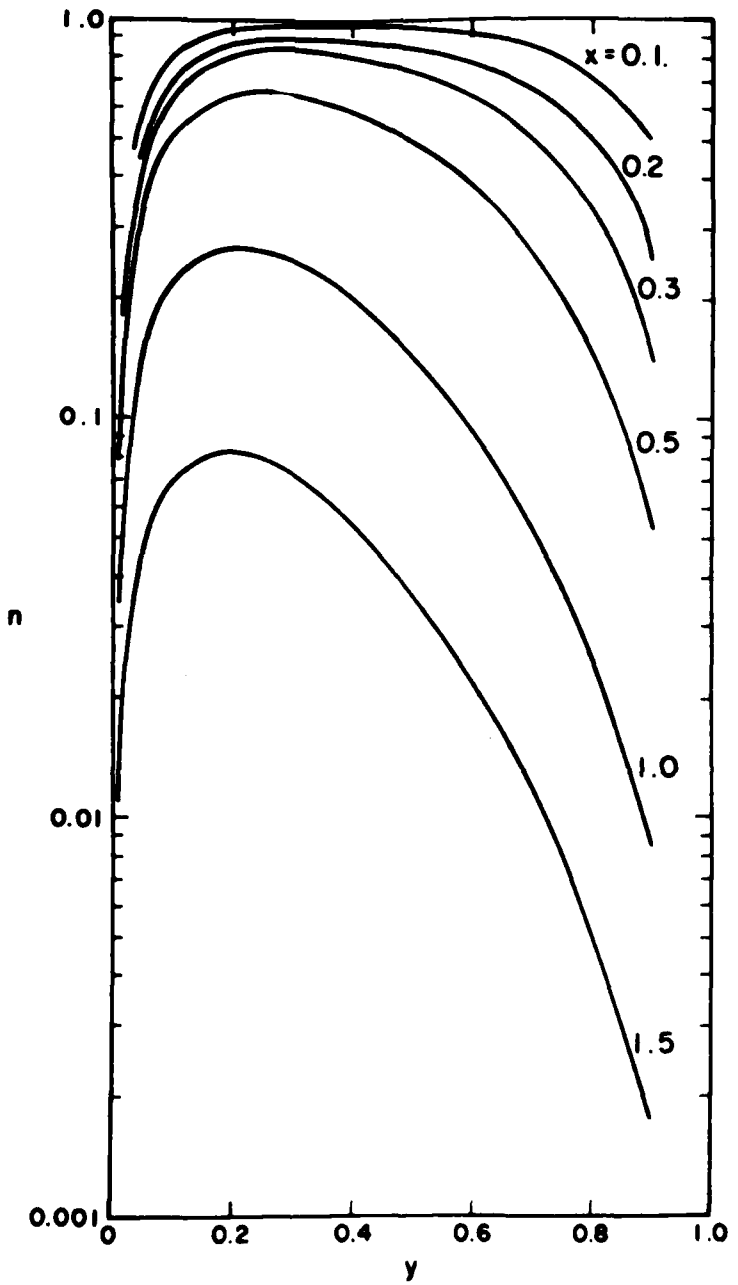

Figure 2-4. Number Density n, vs y With x as a Parameter and $-\rho = \sigma = 10.0$ as Obtained From Series Solution

2.2 Numerical Solution

In this section, we take up solutions of Eq. (2-4) by numerical methods. We do this for two reasons: first, as noted, to extend solutions to larger values of σ and $-\rho$, not attainable by the series solution, and second, to explore methods of solution for more complicated equations for which analytic solutions are not available. Thus, for example, u_o could be a boundary layer flow and v a velocity induced by an electrode with a finite edge leading to non-constant electric fields. Details of the method of solution are presented in Appendix A. As seen from this appendix, the transformation from differential to a difference equation is accomplished in a simple, obvious way. Subsequent tests made for values of σ, $-\rho \leq 60$ indicate that the solution was stable and converging to the correct (series) value; however, the accuracy attained leaves much to be desired. Figure 2-5 shows val-

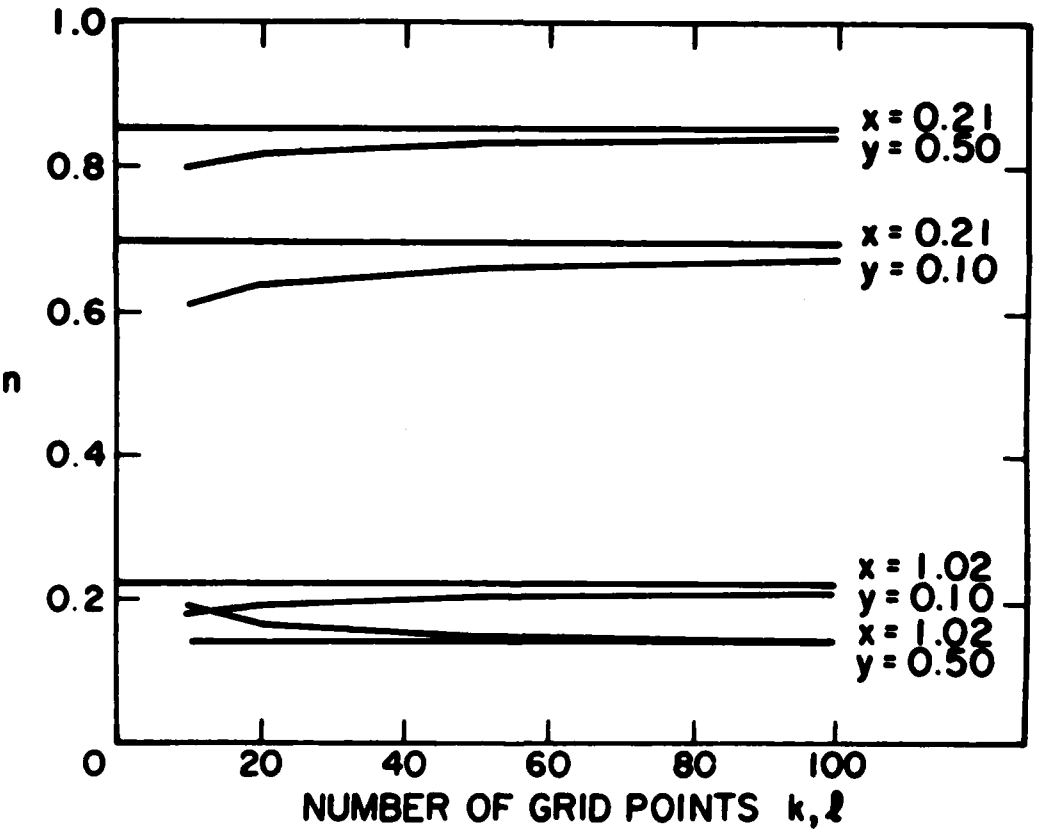

Figure 2-5. Number Density n, vs Number of Grid Points $k = \ell$ for Four Selected Values of (x, y) and $\sigma = -\rho = 10.0$ as Obtained From Numerical Solution

ues of n obtained from the numerical solution for four selected values (x, y), as a function of the number of increments on a side of the grid mesh. An equal number of grid increments in the x and z directions are used. The horizontal lines represent the series solution. The numerical values are seen to be converging towards the series solutions, but even with $k = \ell = 10$, the values for x, y = (0.21, 0.50), (0.21, 0.10), and (1.02, 0.10) differ from the series values by ~3 percent, 2 percent, and 6 percent, respectively. For large values of x, the agreement becomes rapidly worse. Use of more grid points is not feasible because even the 100-by-100 mesh requires ~25 minutes of central processor time on our Cyber 750, and CP time increases as the fourth power of the number of grid increments on a side.

Some results of a numerical solution for $\sigma = -\rho = 100.0$, values not amenable to solution in series form, are shown in Figure 2-6. Here, n is plotted versus x, with y = 0.5 fixed and the number of grid points per side as a parameter. Also plotted on the grid are the results of a perturbation calculation (discussed in Sec-

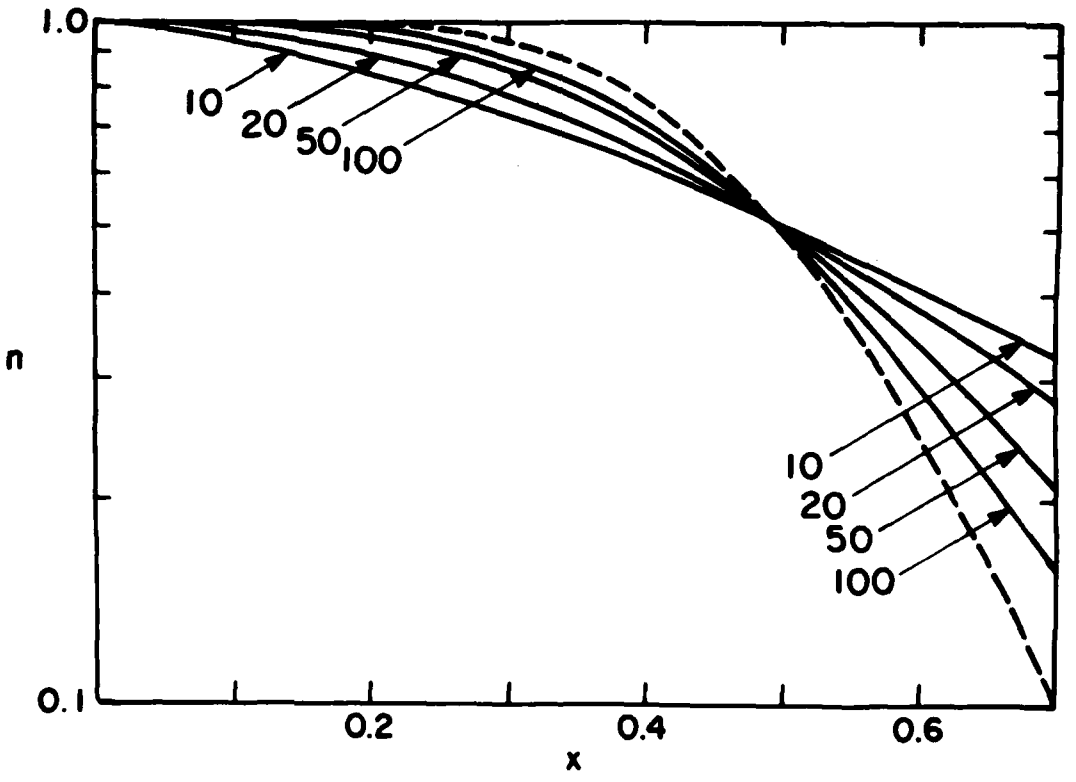

Figure 2-6. Number Density n, vs x for y = 0.5, $\sigma = -\rho = 100$, With $k = \ell$ as a Parameter, as Obtained From Numerical Solution. Dashed curve is the perturbation solution

tion 2.3). We do see, however, that the numerical solution continues to approach the perturbation solution as the number of grid points is increased, an indication of stability if one assumes the perturbation solution to be valid.

The slowness of convergence as well as the lack of accuracy, however, are not reassuring. Before numerical methods such as these can be used to solve flow/diffusion problems, it will be necessary to investigate questions of accuracy and rapidity of convergence with more care.

2.3 Singular (Boundary Layer) Perturbation Solution

For larger values of σ, ρ, we expect that some sort of perturbation method will be applicable in finding solutions of Eq. (2-4). Since the large flow terms are of lower order derivatives than the smaller (diffusion) terms, this will be a singular perturbation problem.[1,2] These problems are not always straightforward to solve, and, in the present instance, we intend to make generous use of intuitive arguments rather than rigor in obtaining a solution.

Zauderer (p. 595) gives a general singular perturbation solution to the following problem, in which ϵ is a small positive quantity.

$$\epsilon\,(u_{xx} + u_{yy}) + u_x + bu_y = 0 \qquad \text{in}$$

$$0 < x < \infty \text{ and } 0 < y < L$$

and b = constant, subject to

$$u(x, o) = f(x);\quad u(o, y) = g(y);\quad u(x, L) = h(x).$$

The solution is

$$u(x, y) \cong h\left(x - \frac{y - L}{b}\right) + \left[f(x) - h\left(x + \frac{L}{b}\right)\right] e^{-(b/\epsilon)y} - \left[g(y) - h\left(\frac{L - y}{b}\right)\right] e^{-x/\epsilon}$$

It is seen immediately that this problem has much in common with the one we are trying to solve. Both the basic partial differential equation, and, if we let L = 1,

---

1. Carrier, George F., and Pearson, Carl E. (1976) Partial Differential Equations, Academic Press, New York.
2. Zauderer, Erich. (1983) Partial Differential Equations of Applied Mathematics, John Wiley & Sons, New York.

the region of investigation, are the same. However, the boundary values in our case, although simple, have certain peculiarities which make it preferable to solve our problem directly without recourse to the general formula. We now proceed to do this.

First, replacing u by n (in accord with our previous notation), the bulk solution (that is, outside of any boundary layer) may be written down by inspection

$$n = \int_{y-1+bx}^{\infty} \delta(x')\, dx' \tag{2-12}$$

where $b = -\rho/\sigma > 0$ and $\delta(x')$ is the Dirac delta function.

We know that there is no boundary at $x = 0$, and, since the flow moves into the region of interest from $y = 1$, there also can be no boundary layer at $y = 1$. Thus, Eq. (2-12) satisfies the boundary conditions $n(0, y) = 1$ and $n(x, 1) = 0$ directly. At $y = 0$, we investigate the possible boundary structure by the stretching transformation.[1,2]

$$y = \varepsilon\eta \tag{2-13}$$

The basic equation

$$\varepsilon (n_{xx} + n_{yy}) - n_x + bn_y = 0 \tag{2-14}$$

then becomes

$$\varepsilon \left(n_{xx} + \frac{1}{\varepsilon^2}\, n_{\eta\eta}\right) - n_x + \frac{b}{\varepsilon}\, n_\eta = 0 \tag{2-15}$$

or to the lowest order in ε

$$n_{\eta\eta} + bn_\eta = 0 \tag{2-16}$$

The boundary conditions for this equation are, with η as the independent variable

$$n(x, o) = 0$$

for $x < 1/b$ and $n(x, \eta) = 0$ for $x > 1/b$

$$n(x, \eta >> 0) = 1$$

A solution of Eq. (2-16) that satisfies the boundary conditions is

$$n(x, \eta) = (1 - e^{-b\eta}) \int_{x - \frac{1}{b}}^{\infty} \delta(x')\, dx' \tag{2-17}$$

The two expressions (2-12) and (2-17) give the density in the bulk region and in the boundary layer, respectively. If, however, we combine the two into

$$n \cong \int_{y - 1 + bx}^{\infty} \delta(x')\, dx' - e^{-\frac{b}{\epsilon} y} \int_{x - 1/b}^{\infty} \delta(x')\, dx' \tag{2-18}$$

we have a single expression which gives the density approximately in the bulk region and also in the boundary layer.

Although Eq. (2-18) is an approximate solution on the external boundaries and throughout the bulk domain of interest, there is still the question of formation of internal boundary layers, and it is clear from the nature of the problem that such an internal boundary layer will exist at $y = 1 - bx$. To investigate this free (internal) boundary, let s = distance normal to $y = 1 - bx$ and t = distance measured from $x = 0$, $y = 1$ along $y = 1 - bx$.

Then the transformation from (x, y) to (t, s) coordinates is given by

$$t = x \frac{1}{\sqrt{1 + b^2}} + (1 - y) \frac{b}{\sqrt{1 + b^2}}$$

$$s = x \frac{b}{\sqrt{1 + b^2}} - (1 - y) \frac{1}{\sqrt{1 + b^2}}$$

The variables may be changed from x, y to s, t in Eq. (2-14) by using the above relations or by observing that the line $y = 1 - bx$ is a characteristic with flow along it and directly applying the equation of continuity. In either case, one obtains

$$\epsilon (n_{ss} + n_{tt}) - \sqrt{1 + b^2}\, n_t = 0 \tag{2-19}$$

If we let (another stretching transformation)

$s = \epsilon^r \eta$, then

$$\varepsilon\left(n_{\eta\eta}\,\frac{1}{\varepsilon^{2r}} + n_{tt}\right) = \sqrt{1+b^2}\; n_t$$

or

$$n_{\eta\eta} + \varepsilon^{2r}\, n_{tt} = \varepsilon^{2r-1}\,\sqrt{1+b^2}\; n_t \tag{2-20}$$

Now, if in Eq. (2-20) we set $r = 1$ and take terms of lowest order in ε, we obtain an equation the solution of which does not have acceptable asymptotic properties. We, therefore, let $r = 1/2$ and obtain to the lowest order in ε

$$n_{\eta\eta} = \sqrt{1+b^2}\; n_t \tag{2-21}$$

Although it is common to obtain an ordinary differential equation for boundary layer solutions, Eq. (2-21) shows that this is not invariably the case. The boundary conditions for Eq. (2-21) are

$n(o, t) = 1/2$ (fixes boundary location)

$$\lim_{\eta >> o} n(\eta, t) = 0$$

$$\lim_{\eta << o} n(\eta, t) = 1$$

$$n(\eta, o) = \int_{\eta}^{\infty} \delta(\eta')\, d\eta'$$

The last of these is based on the argument that at $t = 0$, ions have just entered the region of interest and diffusion cannot have acted to establish a finite boundary layer. Noting that $\mathrm{erf}(-z) = -\mathrm{erf}(z)$ and that $\mathrm{erfc}(z) = 1 - \mathrm{erf}(z)$, we find that the differential equation and all boundary conditions are satisfied by

$$n = 1/2\ \mathrm{erfc}\left[\frac{\eta\,(1+b^2)^{1/4}}{2\sqrt{t}}\right]$$

$$= 1/2\ \mathrm{erfc}\left[\frac{s(1+b^2)^{1/4}}{2\sqrt{\varepsilon\, t}}\right]$$

$$= 1/2 \text{ erfc}\left[\frac{bx - (1 - y)}{2\sqrt{\epsilon}\sqrt{x + b(1 - y)}}\right] \qquad (2\text{-}22)$$

We next observe that the erfc function not only satisfies the free boundary layer requirements, but also for arg (erfc) $<<$ 0 closely approximates the previous bulk solution. Further, the boundary layer equation at $y \cong 0$ is an ordinary equation in y alone: It is still satisfied when multiplied by any arbitrary function of x. We previously chose a delta function to match to the bulk solution at $e^{\frac{b}{\epsilon}y} >> 1$. Now that we have a solution that incorporates the free boundary properties, we may just as easily match the $y \cong 0$ boundary layer to this bulk solution. This results in

$$n = 1/2 \text{ erfc}\left[\frac{bx - (1 - y)}{2\sqrt{\epsilon}\sqrt{x + b(1 - y)}}\right] - e^{-\frac{b}{\epsilon}y} \; 1/2 \text{ erfc}\left[\frac{bx - 1}{2\sqrt{\epsilon}\sqrt{x + b}}\right] \qquad (2\text{-}23)$$

as a final solution. This solution is valid on both boundary layers and throughout the remainder of the domain of interest.

We wish to compare this solution with the series solution, for some larger values of σ, $-\rho$. Since it is fluxes we are mostly concerned with, we take

$$\frac{\partial n}{\partial y}\Big|_{y = 0}$$

to obtain

$$-\rho F = \left(\frac{b}{2\epsilon}\right)\text{erfc}\left[\frac{bx - 1}{2\sqrt{\epsilon}\sqrt{x + b}}\right] - \frac{1}{4\sqrt{\epsilon}} \exp\left[\frac{-(bx - 1)^2}{4\epsilon(x + b)}\right] \frac{x\left(1 + \frac{b^2}{2}\right) + \frac{b}{2}}{(x + b)^{3/2}} \qquad (2\text{-}24)$$

For $\frac{bx - 1}{\sqrt{\epsilon}} << 0$, we have $-\rho F \cong \frac{b}{\epsilon} = -\rho$.

For b = 1, x = 1, and $\epsilon = 1/\sigma = 1/60$,

$-\rho F = 28.6$; the series value is 27.

Figure 2-7 shows a comparison between fluxes obtained from the series solution and from the singular perturbation solution for $\sigma = -\rho = 60$. The agreement is fair, and it is expected that the perturbation values will increase in accuracy with increasing σ, $-\rho$.

Perturbation solutions for n, for $\sigma = -\rho = 100$ and y = 0.5 have already been shown in Figure 2-6.

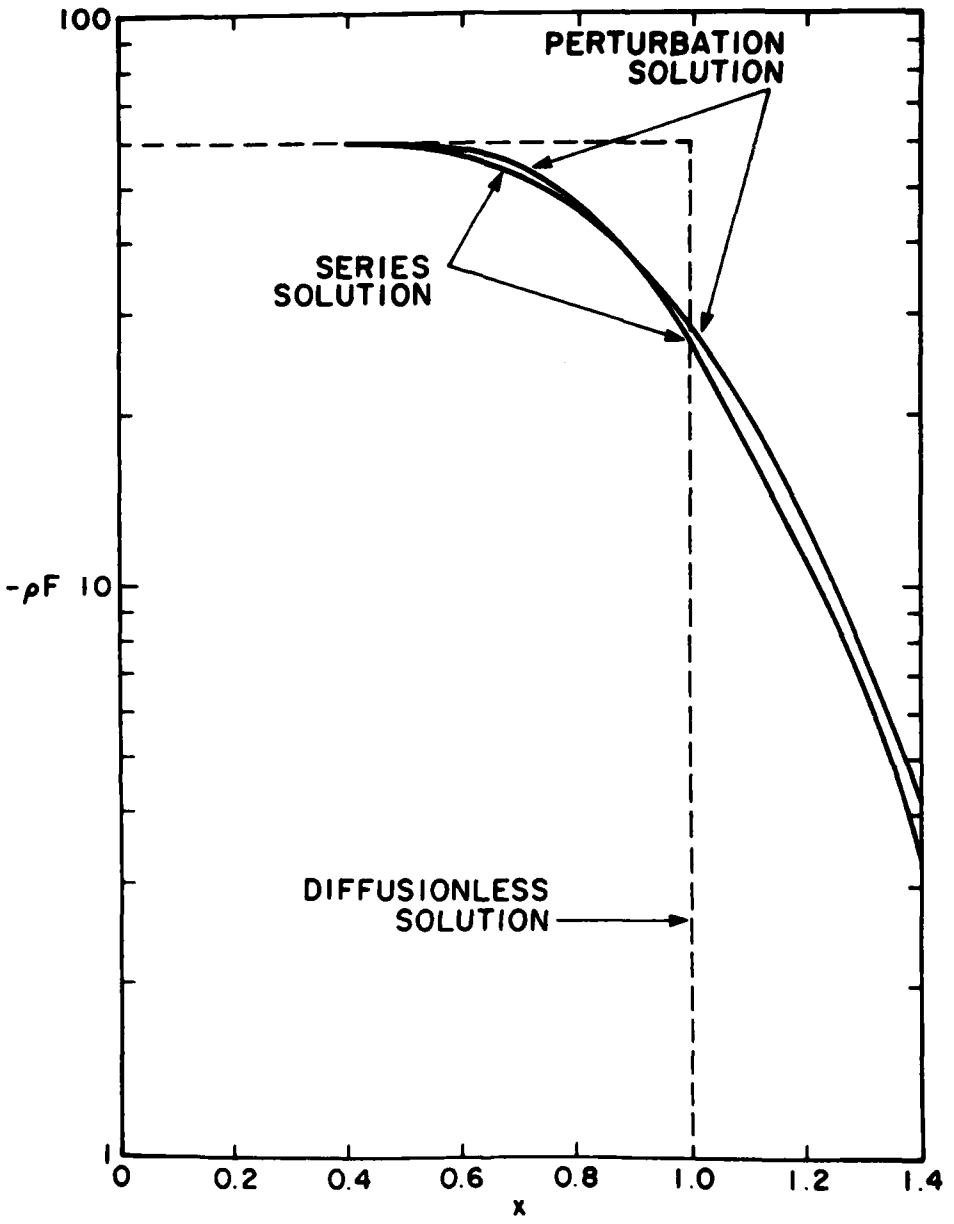

Figure 2-7. Normalized Flux - ρF vs x for $\sigma = -\rho = 60$. Comparison between series values and those obtained from singular perturbation theory

3. DIFFUSION, GENERATION, AND RECOMBINATION WITH SPHERICAL GEOMETRY

Although we have concluded in Section 1 that, in general, diffusion, flow, and mobility are the dominant processes in stratospheric sampling, we here solve a problem that ignores the latter two and includes two other processes of lesser importance. The reason for this is that, whereas flow and/or mobility effects may be completely absent in principle and essentially so on occasion, in practice, diffusion of charged particles cannot be absent when a sampling surface is introduced into a plasma. Thus, in a sense, it underlies all other processes. The solution of a problem of this type is thus informative and, as will be seen, is not too difficult.

We consider the following problem. A sphere collects charged particles by diffusion from a plasma in which both generation and square law recombination occur. It is assumed that there is no charge separation (hence, no electric fields) and a single constant diffusion coefficient. Since generation is by cosmic rays and material bodies are for the most part transparent to cosmic rays, we ignore the effect of the sphere on generation and take the generation rate to be constant as well.

The number density equation for ions undergoing production, recombination, and diffusion in the presence of a spherical collecting surface is

$$D \frac{\partial}{\partial r}\left(r^2 \frac{\partial n'}{\partial r}\right) = \alpha n'^2 - \beta \qquad (3\text{-}1)$$

Here β = production rate (number/cm^3/sec)

α = recombination coefficient (cm^3/sec

r = radial coordinate

and D and n' are as previously defined.

Let $n' = n_o\, y = \sqrt{\alpha/\beta}\, y$

$x = a/r$

$$= \frac{\beta a^2}{n_o D} = \frac{\sqrt{\alpha\beta}\, a^2}{D}$$

where a is the sphere radius.

Then

$$x^4 \frac{d^2 y}{d x^2} = \sigma (y^2 - 1) \qquad (3\text{-}2)$$

The use of σ with a meaning other than that in the previous section will not lead to confusion.

The effect of surface recombination is to fix the number density of charged particles at zero on the surface of the sphere. The boundary conditions are thus

$$y(0) = 1$$

$$y(1) = 0 \qquad (3\text{-}3)$$

Before proceeding to solve Eq. (3-2), it is worth knowing, for actual parameters, what values of σ are likely to be encountered. If, for example, it should turn out that σ is less than, say, 0.01, there is then no need to solve the full equation for, in that event, we have directly $y \cong 1 - x$. Taking typical values from Appendix C, we find that $\sigma/a^2 \cong 0.014/cm^2$ at 20 km and $4 \times 10^{-5}/cm^2$ at 40 km. Since we envision in solving this equation the behavior of the whole sampling platform, we set $a \cong 100$ cm to obtain $\sigma \cong 140$ at 20 km and $\sigma = 0.4$ at 40 km. It is thus clear that it is necessary to solve the full Eq. (3-2).

Eq. (3-2) appears to have a simple form, but the non-linear term precludes solutions in terms of elementary functions, and the equation is not listed in either Kamke[3] or Murphy.[4] We solve it numerically by non-linear relaxation. Relaxation techniques are quite common in solving boundary value problems. However, there do not seem to be many extensive discussions of convergence of non-linear equations. Formally, the extension to this class of problems is straightforward. In the general case, solution of one implicit difference equation is required for each mesh point. For Eq. (3-2), however, solution of implicit equations is not required since the difference equations can be solved explicitly by the quadratic formula. Since the solution is merely formal, however, even though the results do converge, there is no guarantee that:

(1) any solution to the difference equation does, in fact, approach the solution to the original differential equation;

(2) any solution found is unique.

We do not explore either of these two questions here. We do, however, make a minimal effort to insure that the solutions are unique by a variation of the initial values.

---

3. Kamke, E. (1959) Differentialgleichungen Losungsmethoden und Losungen, Chelsea Publishing Co., New York.

4. Murphy, George M. (1960) Ordinary Differential Equations and Their Solutions, D. Van Nostrand Co., Inc., New York.

The results of these calculations are shown in Figure 3-1. Details of the solution are given in Appendix B.

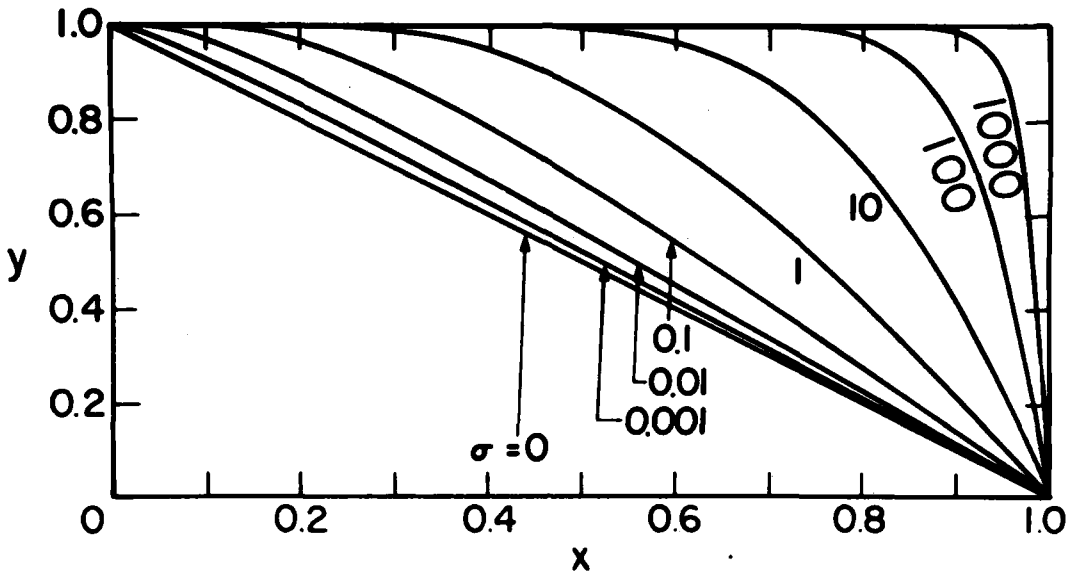

Figure 3-1. Non-Dimensionalized Number Density y vs Non-Dimensionalized Distance x, With σ as Parameter for a Spherical Geometry Without Flow

The form of these solutions, as well as of the Eq. (3-2), suggest that solutions may be approximated by

$$y = 1 - x \exp[\sqrt{\sigma}\ \alpha(1 - 1/x)] \tag{3-4}$$

where α is a constant to be determined. An expression of this form automatically satisfies both boundary conditions and gives an approximate scaling with σ. If Eq. (3-4) is put into Eq. (3-2), there results

$$\alpha^2 - 2 + x \exp[\sqrt{\sigma}\,\alpha\ (1 - 1/x)] = 0 \tag{3-5}$$

We thus have $1 \leq \alpha \leq \sqrt{2}$. We take α to be the geometric mean of these limits, $\alpha = (2)^{1/4}$ and find that Eq. (3-4) agrees with the numerical solutions to within 3 percent for values of $0 < \sigma < 1000$. The comparison is illustrated in Figure 3-2.

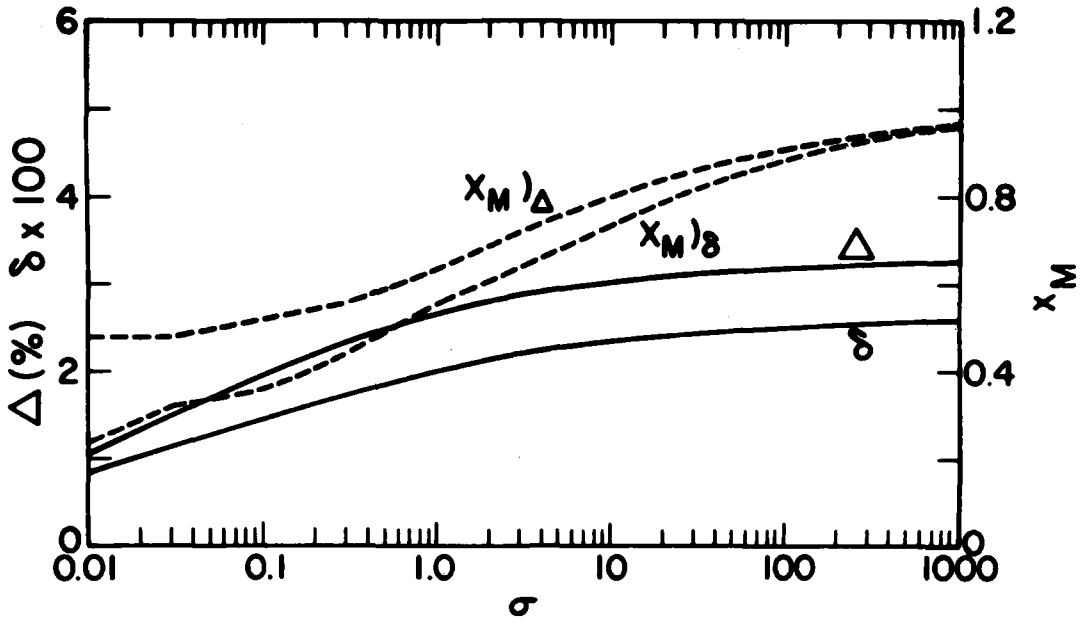

Figure 3-2. Comparison of Numerically Calculated and Empirical Formula Values for Ion Densities as Functions of σ. δ = maximum difference; Δ = maximum relative percent difference; x_{M_δ} = value of x corresponding to δ; x_{M_Δ} = value of x corresponding to Δ

If the numerical values are y_C and the values given by Eq. (3-4) y_F, then the graphs show

$$\delta = (y_C - y_F)_{MAX}$$

and

$$\Delta = \left(\frac{y_C - y_F}{y_C} \right)_{MAX} * 100$$

as functions of σ. Also shown are the corresponding values of x, x_{M_δ}, and x_{M_Δ}.

Of prime interest as far as collection of ions is concerned is the flux to the surface. Because of the accuracy of the approximation in Eq. (3-4), we risk the dangers associated with differentiating approximations and use this formula to obtain the flux. For this purpose, we convert all quantities except σ back to dimensional variables to obtain for the flux

$$D \frac{\partial n}{\partial r} \Bigg)_{r = a} = \frac{Dn_o}{a} (1 + \alpha \sqrt{\sigma}) \qquad (3\text{-}6)$$

The flux to the surface is thus increased by the ratio $(1 + \alpha \sqrt{\sigma})$ over what it would be in the absence of production and recombination near the surface.

References

1. Carrier, George F., and Pearson, Carl E. (1976) Partial Differential Equations, Academic Press, New York.
2. Zauderer, Erich. (1983) Partial Differential Equations of Applied Mathematics, John Wiley & Sons, New York.
3. Kamke, E. (1959) Differentialgleichungen Lösungsmethoden und Lösungen, Chelsea Publishing Co., New York.
4. Murphy, George M. (1960) Ordinary Differential Equations and Their Solutions, D. Van Nostrand Co., Inc., New York.
5. Ames, William F. (1977) Numerical Methods for Partial Differential Equations, Academic Press, New York.

Appendix A

Numerical Solution of Diffusion, Mobility, Flow Equation for Rectangular Geometry

To solve Eq. (2-4) numerically, we first set

$$z = e^{-\alpha x} \tag{A-1}$$

thus mapping the semi-infinite domain $0 \leq x \leq \infty$ into the finite domain $0 \leq z \leq 1$, and transforming Eq. (2-4) into

$$\alpha^2 z^2 \frac{\partial^2 n}{\partial z^2} + \frac{\partial^2 n}{\partial y^2} + \alpha z (\alpha + \sigma) \frac{\partial n}{\partial z} - \rho \frac{\partial n}{\partial y} = 0 \tag{A-2}$$

This is an elliptic equation which we will solve by a relaxation (iterative) method. Numerical values of α are chosen so that $\alpha = O[(\rho/\sigma)]$. This strikes a balance between two extremes related to the value of $n = n_{1,j}$ at the first grid point adjacent to $z = 0$. In one extreme, $n_{1,j}$ is so small as to be of no interest; in the other, $n_{1,j}$ is so large that information is lost.

We next set up a grid as shown in Figure A-1 which also shows values of n on the boundaries.

The most common iteration scheme for solution of partial differential equations uses centered differences for all derivatives. For Eq. (A-2), this results in

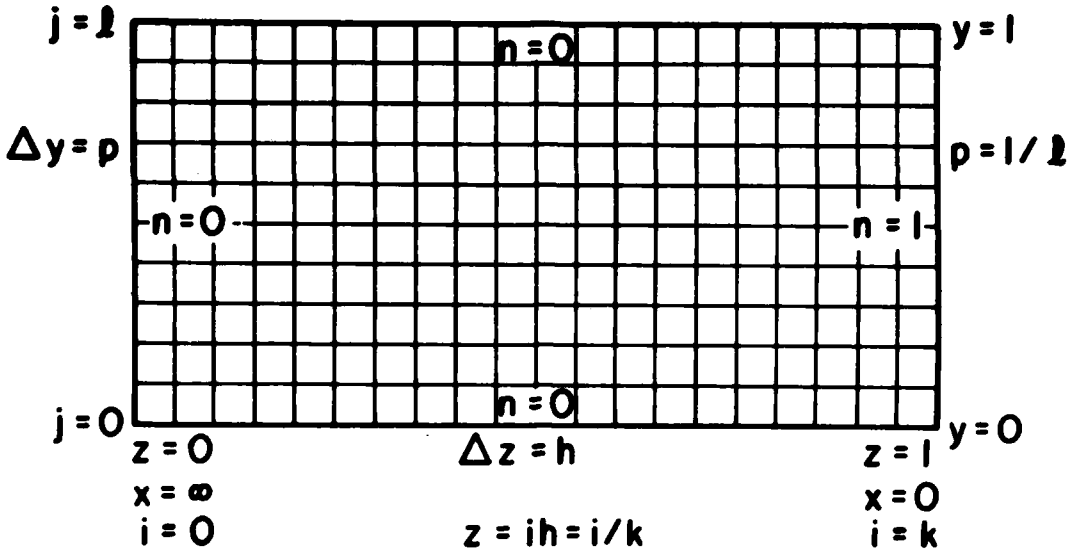

Figure A-1. Calculational Grid Mesh for Numerical Solution of Flow/Diffusion Equation for a Rectangular Geometry; Mesh Has 20-by-10 Increments

$$n_{i,j} = 1/2\,[\,i^2\alpha^2 + \ell^2\,]^{-1} * \left\{ n_{i+1,j}\left(i^2\alpha^2 + \frac{i\alpha}{2}(\alpha+\sigma)\right) + \right.$$

$$\left. n_{i-1,j}\left(i^2\alpha^2 - \frac{i\alpha}{2}(\alpha+\sigma)\right) + n_{i,\,j+1}\left(\ell^2 + \frac{\rho\ell}{2}\right) + n_{i,\,j-1}\left(\ell^2 + \frac{\rho\ell}{2}\right)\right\} \quad \text{(A-3)}$$

with

$$x_i = -(1/\alpha)\ln z_i = -1/\alpha \ln (i/k)$$

This formulation is suspect on two grounds. First, noting that $\rho < 0$, the two terms $n_{i-1,j}\,(i^2\alpha^2 - \frac{i\alpha}{2}(\alpha+\sigma))$ and $n_{i,j-1}\,(\ell^2 + \rho\ell/2)$ will, for sufficiently large σ and $-\rho$, be of the wrong sign to guarantee the existence of unique solutions (Ames,[5] p. 101). Next, suppose we calculate on the first pass the point $i = k - 1$, $j = 1$. Then from the boundary conditions, $n_{i-1,j} = n_{i,\,j+1} = n_{i,\,j-1} = 0$ and $n_{i+1,j} = 1$. From this, $n_{i,\,j} \sim \sigma$ and $n_{i,j}$ can have any value, no matter how large, depending on how large we make σ. Although possibly not fatal, this does not seem like a good prognosis for stability and convergence.

---

5. Ames, William F. (1977) Numerical Methods for Partial Differential Equations, Academic Press, New York.

If, on the other hand, we use centered second differences but forward first differences,

$$\frac{\partial n}{\partial z} \rightarrow ih \ \frac{n_{i+1,j} - n_{i,j}}{h} \ ; \ \frac{\partial n}{\partial y} \rightarrow \frac{n_{i,j+1} - n_{i,j}}{p}$$

we obtain

$$n_{i,j} = (2\, i^2\alpha^2 + 2\ell^2 + i\alpha(\alpha + \sigma) - \rho\ell)^{-1} *$$

$$\Big\{ n_{i+1,j} (i^2\alpha^2 + i\alpha(\alpha + \sigma) + n_{i-1,j}\, i^2\alpha^2$$

$$+ n_{i,j+1} (\ell^2 - \rho\ell) \quad + n_{i,j-1}\, \ell^2 \Big\} \qquad \text{(A-4)}$$

The off diagonal terms now all have the correct sign and $n_{i,j}$ remains of the order unity no matter how large σ and $-\rho$ become. We used Eq. (A-4) for all numerical calculations.

Appendix B

Numerical Solution of Diffusion, Generation, Recombination Equation for Spherical Geometry

Eq. (3-2) may be represented by the following (centered) difference equation:

$$x_j^4 \left(\frac{y_{j+1} - 2y_j + y_{j-1}}{(\Delta x)^2} \right) = \sigma (y_j^2 - 1)$$

Setting $x_j = j\Delta x$ and solving for y_j

$$y_j = 1/\sigma \left\{ -j^4 (\Delta x)^2 \pm \left[j^8 (\Delta x)^4 + \sigma \left(\sigma + j^4 (\Delta x)^2 \ (y_{j+1} + y_{j-1}) \right) \right]^{1/2} \right\} \quad \text{(B-2)}$$

Eq. (B-2) holds for $y_j \neq y_o$, y_m, the two boundary values. For these values, we have $y_o = 1$ and $y_m = 0$. The $\pm$ sign in Eq. (B-2) is chosen + to make $y_j > 0$.

To give some indication of convergence and uniqueness, we solve for each value of σ twice (superscripts are iteration numbers), once with

$$y_j^o = 1, \ j \neq m, \ y_m^o = 0$$

and again with

$$y_j^o = 0, \ j \neq 0, \ y_o^0 = 1.$$

In all cases, the solutions for these two initial conditions continued to approach each other more closely with successive iterations.

Typical values for m were m = 25 and convergence criteria

$$\left(\frac{y_j^{k+1} - y_j^k}{y_j^k} \right)_{\text{MAX}j} \text{ were typically } \sim 10^{-6}.$$

Typically, on the order of several hundred iterations were needed to attain this convergence.

Appendix C

Typical Values for Parameters Occurring in Text

Parameter	Description	20 km	40 km
n_o $(1/cm^3)$	Equilibrium ion density	5500	4000
$\alpha(cm^3/sec)$	Recombination coefficient	5×10^{-7}	5×10^{-8}
$\beta(1/cm^3 sec)$	Ion Production Rate	15	0.75
$\upsilon(cm^3/sec)$	Kinematic Viscosity (μ/ρ)	2	50
V_B (cm/sec)	Platform Drift Velocity	100	100
Re	Drift Reynolds Number	50L	2L
δ(cm)	Drift Boundary Layer Thickness	$\sqrt{L}/7.0$	$\sqrt{L}/1.4$
ρ_o/ρ	Sea Level to Ambient Density Ratio	14	300
λ(cm)	Neutral-neutral Mean Free Path	9×10^{-5}	2×10^{-3}
L (cm)	Characteristic Dimension	100 for platform	

END

DTIC

8-86